Subretinal Drusenoid Deposits and Photoreceptor Loss Detecting Global and Local Progression of Geographic Atrophy by SD-OCT Imaging

Gregor S. Reiter,[1,2] Reinhard Told,[2] Markus Schranz,[2] Lukas Baumann,[3] Georgios Mylonas,[2] Stefan Sacu,[2] Andreas Pollreisz,[2] and Ursula Schmidt-Erfurth[1,2]

[1]Christian Doppler Laboratory for Ophthalmic Image Analysis, Vienna Reading Center, Department of Ophthalmology and Optometry, Medical University of Vienna, Vienna, Austria
[2]Vienna Clinical Trial Center (VTC), Department of Ophthalmology and Optometry, Medical University of Vienna, Vienna, Austria
[3]Center for Medical Statistics, Informatics and Intelligent Systems, Medical University of Vienna, Vienna, Austria

Correspondence: Andreas Pollreisz, Department of Ophthalmology and Optometry, Medical University of Vienna, Währinger Gürtel 18-20, 1090 Vienna, Austria; andreas.pollreisz@meduniwien.ac.at.

Received: December 26, 2019
Accepted: May 12, 2020
Published: June 5, 2020

Citation: Reiter GS, Told R, Schranz M, et al. Subretinal drusenoid deposits and photoreceptor loss detecting global and local progression of geographic atrophy by SD-OCT imaging. *Invest Ophthalmol Vis Sci.* 2020;61(6):11. https://doi.org/10.1167/iovs.61.6.11

Purpose. To investigate the impact of subretinal drusenoid deposits (SDD) and photoreceptor integrity on global and local geographic atrophy (GA) progression.

Methods. Eighty-three eyes of 49 patients, aged 50 years and older with GA secondary to age-related macular degeneration (AMD), were prospectively included in this study. Participants underwent spectral-domain optical coherence tomography (SD-OCT) and fundus autofluorescence (FAF) imaging at baseline and after 12 months. The junctional zone and presence of SDD were delineated on SD-OCT and FAF images. Linear mixed models were calculated to investigate the association between GA progression and the junctional zone area, baseline GA area, age, global and local presence of SDD and unifocal versus multifocal lesions.

Results. The area of the junctional zone was significantly associated with the progression of GA, both globally and locally (all $P < 0.001$). SDD were associated with faster growth in the overall model ($P = 0.039$), as well as in the superior-temporal ($P = 0.005$) and temporal ($P = 0.002$) sections. Faster progression was associated with GA baseline area ($P < 0.001$). No difference was found between unifocal and multifocal lesions ($P > 0.05$). Age did not have an effect on GA progression ($P > 0.05$).

Conclusions. Photoreceptor integrity and SDD are useful for predicting global and local growth in GA. Investigation of the junctional zone is merited because this area is destined to become atrophic. Photoreceptor loss visible on SD-OCT might lead to new structural outcome measurements visible before irreversible loss of retinal pigment epithelium occurs.

Keywords: age-related macular degeneration, photoreceptor integrity, reticular pseudodrusen, retinal pigment epithelium, subretinal drusenoid deposits

Geographic atrophy (GA) is the late stage of nonneovascular age-related macular degeneration (AMD) and is characterized by the loss of retinal pigment epithelium (RPE), photoreceptors and choriocapillaris with characteristic extracellular deposits between outer retinal cells and their blood supply.[1–4] Growth of GA lesions, which are usually graded on color fundus photographs or in fundus autofluorescence (FAF) imaging, is progressive, and ranges from 1.2 mm^2 to 2.6 mm^2 per year.[5–9] The enlargement of GA is the only structural endpoint approved by regulatory agencies; however, efforts are made to find earlier endpoints.[10–12] Various prognostic factors, such as GA baseline area without square root transformation or bilateral GA lesions, have been identified in observational cohort studies revealing patients at risk for faster disease progression.[6,9] Spectral-domain optical coherence tomography (SD-OCT) imaging exhibits excellent correlation with FAF-based measurements for GA,[13] and enlargement rates showed good interobserver agreement when measured with FAF or SD-OCT.[6,14,15]

The junctional zone, the transitional area surrounding the GA lesion, has undergone various definitions focusing either on anatomic changes or on fixed margins.[16–18] In histologic studies the external limiting membrane (ELM) descent demarcates the edge of the atrophic area with the transition into the junctional zone.[19] Photoreceptor defects and stacked RPE cells are present demarcating the subsequent area to become atrophic.[20] A highly variable FAF pattern is observed in the junctional region. This pattern is not thought to be due to intracellular lipofuscin accumulation but caused by stacked RPE.[3,21]

Recently, reticular pseudodrusen (RPD) have gained attention in retinal studies. These subretinal deposits are also known as subretinal drusenoid deposits (SDD).[22] These deposits are found internal and adjacent to the RPE and

might disturb the ellipsoid zone anatomy when investigated on OCT images.[23,24] SDD show a distinct lifecycle with initial growth and subsequent regression in which SDD can be classified in a three-stage grading system.[23,25] In its greatest extent, the SDD disrupts the ellipsoid zone and is classified as stage 3.[23] Initially RPD and SDD were not considered the same entity. RPD were visible on blue reflectance photographs, infrared, and FAF images, whereas SDD were described on OCT B-scans. However, multimodal imaging proved RPD and SDD to be the same structure.[23] Eyes with SDD are at higher risk for the progression to both neovascular and nonneovascular late stage AMD.[26–28] In nonneovascular AMD a high correlation was demonstrated between fields with SDD at baseline and subsequent GA progression.[26,27] In neovascular AMD SDD double the risk of neovascular progression over soft drusen alone.[28] Also, eyes with nonneovascular AMD often exhibit SDD, which have a higher prevalence in the superior-temporal perifovea, spatially coinciding with higher rod densities which show their highest density in an elliptical ring surrounding the fovea with a peak approximately superior to the fovea.[29–31] This study aimed to investigate the impact of SDD, as well as global and local photoreceptor integrity loss delineating the junctional zone on the progression of geographic atrophy.

Methods

Consecutive patients with GA were enrolled in this prospective cohort study, which was approved by the Ethics Committee of the Medical University of Vienna. All patients gave written informed consent before inclusion. The study adhered to the Declaration of Helsinki and the Good Clinical Practice (GCP) guidelines. Patients with GA secondary to AMD with either unifocal or multifocal lesions were included in this study; hence, patients with foveal sparing were also included. The absence or presence of SDD on FAF and SD-OCT was not a study inclusion criterion. Patients with a history of choroidal neovascularization (CNV) or who had had anti-vascular endothelium growth factor (VEGF) injections were excluded. Both eyes were included if eligible, and this was incorporated in the statistical model.

Study visits included a baseline and 12-month follow-up visit. Best-corrected visual acuity (BCVA) was tested using the Early Treatment Diabetic Retinopathy Study (ETDRS) chart. A complete ophthalmologic examination including funduscopy after pupil dilation with 0.5% tropicamide and 2.5% phenylephrine to at least 7 mm diameter was performed. Infrared images, fundus autofluorescence (FAF) images, and spectral domain optical coherence tomography (SD-OCT) (Spectralis HRA+OCT Heidelberg Engineering, Heidelberg, Germany) were acquired after pupil dilation.

SD-OCT Imaging Protocol

A volume comprising the central 6x6mm was acquired with a resolution of 1024 x 49 (A-scans x B-scans; Spectralis HRA+OCT Heidelberg Engineering). At the baseline visit, the scan was carefully centered on the fovea or if no fovea was clearly detectable the scan was focused to cover the entire atrophic area and the system's follow-up mode was used at the 12-month follow-up visit to reacquire the OCT image. All volume scans were exported for manual marking of the SDD and junctional zone.

Marking of SD-OCT Findings and SDD

The GA lesion was delineated on FAF images pursuant to the current FDA approved gold standard.[12] The growth area of GA was defined on FAF as the area between the delineation border at baseline and after one year as described previously [32] (see Figs. 1E, 1F). SD-OCT volume scans were imported into validated reading center software (OCTAVO; Vienna Reading Center, Vienna, Austria). For the purpose of this study, we defined the border of the junctional zone by the integrity of the photoreceptors, which we marked corresponding to the loss of the ellipsoid zone on each SD-OCT B-scan (see Figs. 2A, 2B). The manually delineated area was transferred to the registered infrared image and finally transferred to the FAF image after a three-point image registration was performed (see Supplementary Video). The junctional zone was then defined as the area between the borders of the baseline GA FAF image and the baseline SD-OCT junctional zone (see Figs. 1C, 1D). The delineated area was divided into eight sections, which converged at the fovea (see Fig. 1), to assess the local kinetics. The presence of SDD was evaluated on FAF images and SD-OCT B-scans and annotated globally for each eye, as well as for each octant.

Statistics

A primary linear mixed model was computed with the GA growth area as the dependent and baseline GA area, baseline junctional zone area, age, the presence of SDD and GA configuration (unifocal and multifocal) as independent variables. Patient- and eye-specific random intercepts could be specified (the eye-specific random effect was nested in the patient-specific random effect) because both eyes were measured in most patients and measurements in the eye were divided into eight sections. To further investigate GA growth based on the different topographic distribution of SDD,[30] the same model was computed eight times for each section of the eye, but only with patient-specific random intercepts (eye-specific random intercepts were not necessary because there was only one value per eye in each section).

Furthermore, another mixed model was computed to test whether the mean BCVA changed from baseline to one year, with the change in BCVA (1-year minus baseline value) as the dependent variable and only the intercept as an explanatory variable. Again, patient-specific random intercepts were specified. The level of statistical significance was set at $\alpha = 0.05$. Estimates were derived from the statistical model and were calculated as mm^2 change of growth per mm^2 of GA growth per 12 months. The primary analysis was calculated first and the section analysis might be seen as an explorative subgroup analysis to assess the impact of SDD distribution, hence, no correction for multiple testing was implemented.

Results

Eighty-three eyes of 49 patients were included. Twenty-two eyes (27.7%) were from male participants. The patients' mean age at baseline was 76.4 ± 7.8 years (Table 1). Fifty-four eyes (65.1%) presented with a unifocal GA lesion. Fifty-nine (71.1%) eyes had SDD. The presence of SDD was further noted for each octant segment. SDD were found in 46 eyes in the inferior section, in 44 eyes in the inferior-nasal section, in 45 eyes in the inferior-temporal section, in 44

Investigative Ophthalmology & Visual Science

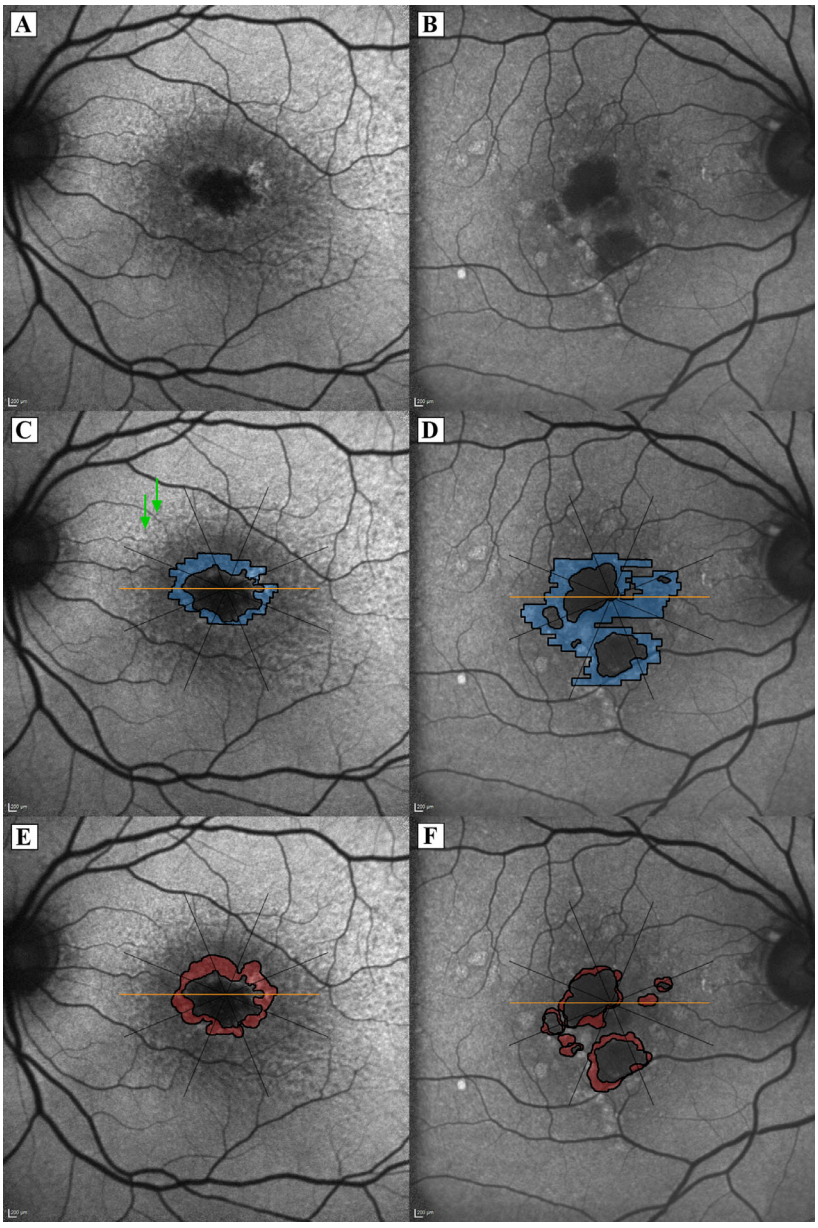

Figure 1. Fundus autofluorescence (FAF) imaging and demarcation of the junctional zone (*blue*) and growth area (*red*) in unifocal and multifocal geographic atrophy (GA); (**A, B**) FAF images without overlays. (**C, D**) the junctional zone (*blue*) defined as the area between the border of the baseline GA (FAF image) and the baseline spectral-domain optical coherence tomography junctional zone border; (**E, F**) growth area (*red*) as the area between FAF GA lesion delineation at baseline and follow-up. Subretinal drusenoid deposits (SDD) are visible in all octants in the eye with unifocal GA (Left column; note the typical dot-like appearance of SDD and *green arrows* exemplarily indicate SDD in the superior-nasal section).

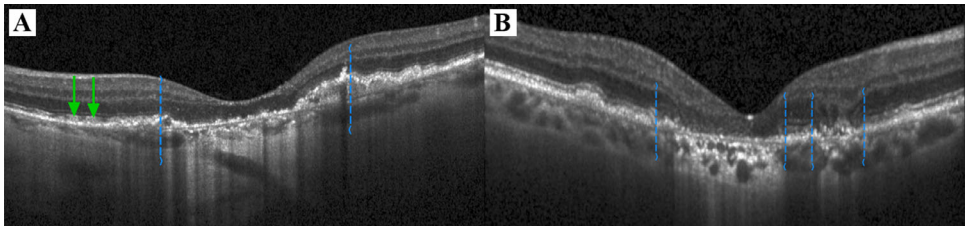

Figure 2. Markings of the junctional zone borders in unifocal (**A**) and multifocal geographic atrophy (**B**); Borders of ellipsoid zone loss on spectral-domain optical coherence tomography (SD-OCT) indicating the outer edges of the junctional zone (*blue dashed lines*; B-scan of the SD-OCT corresponding to Figure 1); *Green arrows* in **A** mark the presence of small subretinal drusenoid deposits (SDD).

Investigative Ophthalmology & Visual Science

Table 1. Summary of Demographics and Clinical Features for the Entire Cohort

Data Type	Data
Patients demographics	
Age (yrs), mean (SD)	76.4 (7.8)
Male sex, no. (%)	22 (27.7)
Clinical features	
Unifocal GA, no. (%)	54 (65.1)
SDD, no. (%)	59 (71.1)
Baseline GA area (mm^2), mean (SD)	6.1 (4.4)
GA growth area (mm^2), mean (SD)	1.5 (1.0)
Baseline junctional zone area (mm^2), mean (SD)	2.3 (1.4)
Baseline BCVA (logMAR), mean (SD)	0.46 (0.36)

BCVA, best corrected visual acuity; GA, geographic atrophy; logMAR, logarithm of the minimum angle of resolution; SD, standard deviation; SDD, subretinal drusenoid deposits.

Table 2. Presence of SDD Per Eye and Each Section Separately

Sections	Presence of SDD, no. (%)
Overall	59 (71.1)
Nasal	44 (53)
Superior-nasal	50 (60.2)
Superior	55 (66.3)
Superior-temporal	55 (66.3)
Temporal	46 (55.4)
Inferior-temporal	45 (54.2)
Inferior	46 (55.4)
Inferior-nasal	44 (53)

SDD, subretinal drusenoid deposits.

eyes in the nasal section, in 55 eyes in the superior section, in 50 eyes in the superior nasal section, in 55 eyes in the superior-temporal section, and in 46 eyes in the temporal section (Table 2). The mean GA area at baseline was 6.1 ± 4.4 mm^2. After 12 months of follow-up the GA lesion enlarged by 1.5 ± 1.0 mm^2. The mean baseline junctional zone area was 2.3 ± 1.4 mm^2.

Mean BCVA worsened from 0.46 ± 0.36 logarithm of the minimum angle of resolution (logMAR) (Snellen equivalent approximately 20/58) to 0.56 ± 0.37 logMAR (Snellen equivalent approximately 20/73) ($P < 0.001$) over 12 months.

In the overall model, the GA growth after 12 months was significantly associated with the area of the junctional zone at baseline ($P < 0.001$; estimate = 0.461), GA area at baseline ($P < 0.001$; estimate = 0.049) and the global presence of SDD ($P = 0.039$; estimate = 0.049). Age did not have an effect on GA growth ($P > 0.05$), and no difference in GA growth could be found between unifocal and multifocal lesions ($P > 0.05$). Because there was no difference between unifocal and multifocal lesions, all results were pooled (Table 3).

In the sectorial analyses, the junctional zone area was always significantly associated with GA growth ($P < 0.001$ for all eight sections; estimate range = 0.332–0.641). The GA baseline area was significantly associated with GA growth in the inferior ($P = 0.018$; estimate = 0.063) and nasal section ($P = 0.029$; estimate = 0.066). No association was found in the other six sections (all $P > 0.05$). SDD was locally associated with GA growth in the superior-temporal ($P = 0.005$; estimate = 0.108) and temporal sections ($P = 0.002$; estimate = 0.077). A trend was identified in the superior section ($P = 0.066$; estimate = 0.07), but no association was found in the other five sections (all $P > 0.05$). Age was associated with GA growth in the superior ($P = 0.006$; estimate = −0.007), superior-nasal ($P = 0.035$; estimate = −0.004) and superior-temporal sections ($P = 0.005$; estimate = −0.007). No association was found in the other five sections (all $P > 0.05$). A difference between unifocal and multifocal growth was only observed in the superior section ($P = 0.015$; estimate = 0.098 for multifocal GA; for all other sections $P > 0.05$).

Discussion

Photoreceptor loss, leading to an increasing field loss, is one of the main features of GA.[1] Visual acuity impairment depends strongly on the integrity of the foveal photoreceptors, which is referenced as foveal sparing. The loss of RPE and depletion of intact overlying photoreceptors in the fovea lead to an irreversible vision loss.[33] Current studies focus on the lesion growth as a structural endpoint of GA, which is measurable on FAF imaging.[10] SD-OCT is now widely available and the three-dimensional data acquired provides information about the course of disease additional to that from conventional two-dimensional FAF imaging.[34] In particular, the area soon to become atrophic, the so-called junctional zone, may be an accurate predictor of GA growth, as this study has proven. This is not only true for the global enlargement in both unifocal and multifocal GA lesions but also for each sub-section (all $P < 0.001$). It might therefore be an earlier indicator of GA progression than the irreversible and already occurred complete loss of RPE detectable with FAF. The calculated estimate indicates that the GA lesion will grow 0.461 mm^2 per 1 mm^2 of junctional zone (section range 0.332–0.641 mm^2) per year. This indicator could become

Table 3. Estimates (mm^2 Change of Growth Per mm^2 of GA Growth Per 12 Months) and *P* Values of the Mixed Models for the Overall Eye and Each Section Separately

Sections	Baseline Junctional Zone Area	Baseline GA Area	Age	SDD	Configuration (Multifocality)
Overall	0.461 ($P < 0.001$)	0.049 ($P < 0.001$)	−0.002 ($P = 0.104$)	0.045 ($P = 0.039$)	0.026 ($P = 0.24$)
Nasal	0.332 ($P < 0.001$)	0.066 ($P = 0.029$)	−0.001 ($P = 0.669$)	0.017 ($P = 0.585$)	−0.004 ($P = 0.91$)
Superior-nasal	0.406 ($P < 0.001$)	0.038 ($P = 0.157$)	−0.004 ($P = 0.035$)	0.018 ($P = 0.547$)	0.047 ($P = 0.151$)
Superior	0.614 ($P < 0.001$)	0.04 ($P = 0.14$)	−0.007 ($P = 0.006$)	0.007 ($P = 0.066$)	0.098 ($P = 0.015$)
Superior-temporal	0.641 ($P < 0.001$)	−0.001 ($P = 0.964$)	−0.007 ($P = 0.005$)	0.108 ($P = 0.005$)	−0.028 ($P = 0.464$)
Temporal	0.338 ($P < 0.001$)	0.019 ($P = 0.456$)	0 ($P = 0.895$)	0.077 ($P = 0.002$)	0.032 ($P = 0.235$)
Inferior-temporal	0.36 ($P < 0.001$)	0.022 ($P = 0.425$)	−0.003 ($P = 0.171$)	0.032 ($P = 0.248$)	0.039 ($P = 0.229$)
Inferior	0.403 ($P < 0.001$)	0.063 ($P = 0.018$)	0.002 ($P = 0.204$)	0.018 ($P = 0.468$)	0.019 ($P = 0.51$)
Inferior-nasal	0.5 ($P < 0.001$)	0.039 ($P = 0.15$)	0.003 ($P = 0.066$)	0.024 ($P = 0.364$)	−0.006 ($P = 0.846$)

GA, geographic atrophy; SDD, subretinal drusenoid deposits.

Investigative Ophthalmology & Visual Science

helpful in studies investigating growth-decelerating treatments or for detecting progression even before RPE loss occurs.

Another finding of this study was an association between the GA baseline area and the growth area after 12 months ($P < 0.001$ in the overall model). This association became statistically significant only in the superior and inferior sections ($P = 0.029$ and $P = 0.018$, respectively) when assessing local kinetics. It has to be noted that we did not apply a square root transformation to our data, which could alter this result, but it is an already well-explained finding.[6] Over the last decade SDD have become a well-known risk factor for the progression to late AMD stages, particularly GA.[22,26,27] We proved that SDD are not only a risk factor for the progression to late AMD but also accelerate GA growth. The global estimate indicates larger growth by 0.049 mm^2 per mm^2 lesion growth per year (approximately +5%) if the affected eye has SDD. Interestingly, we also found an association in the superior-temporal ($P = 0.005$; estimate = 0.108) and temporal sections ($P = 0.002$; estimate = 0.077) and a trend in the superior section ($P = 0.066$; estimate = 0.07), which are topographically the sections with the most common appearance of SDD.[30] If present in these sections, SDD might also accelerate GA enlargement. However, no statistical significance was reached in the other sections where SDD are not as frequent.[30] In addition to our study, an even stronger association between SDD and GA progression was found by Xu et al.,[26] which may indicate a common pathophysiology between SDD and SDD-related GA. With the advances in artificial intelligent (AI), the real potential of these hardly comprehensible masses of data points generated daily by SD-OCT can be realized,[35,36] and the investigation of SDD will continuously enrich our understanding of AMD.

Other studies focusing on the natural progression of GA found GA growth best describable by a linear enlargement of the lesion radius.[37] However, concentric growth rates differ with growth accelerated in the parafovea with a significant decrease outside the macula.[38] This finding is in agreement with the decelerated growth of GA in larger lesions.[39] In addition, stacked RPE cells may build up at the immediate border of GA and contribute to the appearance of various hyperautofluorescence patterns and associated changes in growth rates.[40] Although significant in qualitative assessments, our group found only a partial association between quantitative autofluorescence and GA progression in solitary GA.[32] Compared to the cited studies, the study presented here investigated topographic differences based on the topographic distribution of SDD. Different to the recent report of the AREDS2 study group,[9] our results revealed no faster growth of multifocal than of unifocal lesions. This might be due to the large number of unifocal lesions in this study (54 eyes against 29 eyes). Previously reported prevalence of multifocal lesions revealed a much higher number of multifocal lesions, even more when including coalescent multifocal lesions.[26] The number of unifocal GA in this study is higher, because patients that convert from intermediate to atrophic AMD in the early and intermediate AMD study at the Vienna Clinical Trial Center are switched to the study investigated here. Therefore the prevalence of smaller, unifocal lesions are high in this investigation, and coalescence is more infrequent. However, our current study did not primarily investigate the differences between lesion types, but rather SDD as part of the pathomechanism of GA progression. Because this might not represent the exact proportion in atrophic AMD, this has to be accepted as a limitation of the study. This study investigated the impact of SDD on GA growth; however, we did not quantify the amount of SDD. This could nevertheless be of benefit for understanding SDD, and AI might be best suited to automatically detect, count, and quantify SDD in further analyses.[41] For the purpose of this study, we did not differentiate between growth towards the periphery and the fovea, which has already been shown to be different in eyes with GA sparing the fovea.[42] We do not consider this to have a strong impact on the results of this study because growth is slow towards the fovea (one tenth of the growth towards the periphery[42]). Furthermore, ocular magnification may differ inter-individually, which may alter area measurements. Therefore the stated values might not be absolute, which has to be accepted as a limitation. The involvement of choroidal and choriocapillary vessel changes in the pathophysiology of GA was reported[4,43]; however, this additional issue was not part of this study's investigation. Future studies will have to combine vascular changes with OCT structural findings. The exploratory subgroup analysis of this study included the investigation of eight topographic sections and we decided not to correct for multiple testing. Because these exploratory model were computed eight times, the possibility of an error due to multiple comparison is existent and must be accepted as a limitation.

In conclusion, we found a strong impact of global and local junctional zone area measurements on the progression of GA, which enables to predict global and local growth before irreversible RPE loss occurs. The presence of SDD proved to have an accelerating effect on GA progression, both globally and locally in sections that most commonly have SDD. Studies that focus on quantifying the number and volume of SDD promise to make a valuable contribution to our understanding of these deposits in the natural course of non-neovascular AMD.

Acknowledgments

Disclosure: **G.S. Reiter,** None; **R. Told,** None; **M. Schranz,** None; **L. Baumann,** None; **G. Mylonas,** None; **S. Sacu,** None; **A. Pollreisz,** None; **U. Schmidt-Erfurth,** None

References

1. Sunness JS. The natural history of geographic atrophy, the advanced atrophic form of age-related macular degeneration. *Mol Vis*. 1999;5:25.
2. Bonilha VL. Age and disease-related structural changes in the retinal pigment epithelium. *Clin Ophthalmol*. 2008;2:413–424.
3. Zanzottera EC, Ach T, Huisingh C, Messinger JD, Spaide RF, Curcio CA. Visualizing retinal pigment epithelium phenotypes in the transition to geographic atrophy in age-related macular degeneration. *Retina*. 2016;36(Suppl 1):S12–S25.
4. Li M, Huisingh C, Messinger J, et al. Histology of geographic atrophy secondary to age-related macular degeneration. *Retina*. 2018;38:1937–1953.
5. Lindblad AS, Lloyd PC, Clemons TE, et al. Change in area of geographic atrophy in the Age-Related Eye Disease Study: AREDS report number 26. *Arch Ophthalmol (Chicago, Ill 1960)*. 2009;127:1168–1174.
6. Yehoshua Z, Rosenfeld PJ, Gregori G, et al. Progression of geographic atrophy in age-related macular degeneration imaged with spectral domain optical coherence tomography. *Ophthalmol*. 2011;118:679–686.

7. Sunness JS, Margalit E, Srikumaran D, et al. The long-term natural history of geographic atrophy from age-related macular degeneration: enlargement of atrophy and implications for interventional clinical trials. *Ophthalmol*. 2007;114:271–277.
8. Klein R, Meuer SM, Knudtson MD, Klein BEK. The epidemiology of progression of pure geographic atrophy: the Beaver Dam Eye Study. *Am J Ophthalmol*. 2008;146:692–699.
9. Keenan TD, Agrón E, Domalpally A, et al. Progression of Geographic Atrophy in Age-related Macular Degeneration: AREDS2 Report Number 16. *Ophthalmol*. 2018;125:1913–1928.
10. Schaal KB, Rosenfeld PJ, Gregori G, Yehoshua Z, Feuer WJ. Anatomic Clinical Trial Endpoints for Nonexudative Age-Related Macular Degeneration. *Ophthalmol*. 2016;123:1060–1079.
11. Guymer RH, Rosenfeld PJ, Curcio CA, et al. Incomplete Retinal Pigment Epithelial and Outer Retinal Atrophy in Age-Related Macular Degeneration. *Ophthalmol*. 2020;127:394–409.
12. Csaky K, Ferris F, Chew EY, Nair P, Cheetham JK, Duncan JL. Report From the NEI/FDA Endpoints Workshop on Age-Related Macular Degeneration and Inherited Retinal Diseases. *Invest Opthalmol Vis Sci*. 2017;58:3456.
13. Simader C, Sayegh RG, Montuoro A, et al. A longitudinal comparison of spectral-domain optical coherence tomography and fundus autofluorescence in geographic atrophy. *Am J Ophthalmol*. 2014;158:557–566.
14. Panthier C, Querques G, Puche N, et al. Evaluation of semiautomated measurement of geographic atrophy in age-related macular degeneration by fundus autofluorescence in clinical setting. *Retina*. 2014;34:576–582.
15. Sadda SR, Chakravarthy U, Birch DG, Staurenghi G, Henry EC, Brittain C. Clinical Endpoints for the Study of Geographic Atrophy Secondary To Age-Related Macular Degeneration. *Retina*. 2016;36:1806–1822.
16. Allingham MJ, Nie Q, Lad EM, et al. Semiautomatic Segmentation of Rim Area Focal Hyperautofluorescence Predicts Progression of Geographic Atrophy Due to Dry Age-Related Macular Degeneration. *Invest Ophthalmol Vis Sci*. 2016;57:2283–2289.
17. Hwang JC, Chan JWK, Chang S, Smith RT. Predictive value of fundus autofluorescence for development of geographic atrophy in age-related macular degeneration. *Invest Ophthalmol Vis Sci*. 2006;47:2655–2661.
18. Qu J, Velaga SB, Hariri AH, Nittala MG, Sadda S. Classification and quantitative analysis of geographic atrophy junctional zone using spectral domain optical coherence tomography. *Retina*. 2018;38:1456–1463.
19. Li M, Dolz-Marco R, Huisingh C, et al. Clinicopathologic correlation of geographic atrophy secondary to age-related macular degeneration. *Retina*. 2019;39:802–816.
20. Sarks JP, Sarks SH, Killingsworth MC. Evolution of geographic atrophy of the retinal pigment epithelium. *Eye*. 1988;2:552–577.
21. Rudolf M, Vogt SD, Curcio CA, et al. Histologic basis of variations in retinal pigment epithelium autofluorescence in eyes with geographic atrophy. *Ophthalmol*. 2013;120:821–828.
22. Spaide RF, Ooto S, Curcio CA. Subretinal Drusenoid Deposits AKA Pseudodrusen. *Surv Ophthalmol*. 2018;63:782–815.
23. Zweifel SA, Spaide RF, Curcio CA, Malek G, Imamura Y. Reticular Pseudodrusen Are Subretinal Drusenoid Deposits. *Ophthalmol*. 2010;117:303–312.e1.
24. Zhang Y, Wang X, Rivero EB, et al. Photoreceptor perturbation around subretinal drusenoid deposits as revealed by adaptive optics scanning laser ophthalmoscopy. *Am J Ophthalmol*. 2014;158:584–596.e1.
25. Zhang Y, Wang X, Sadda SR, et al. Lifecycles of individual subretinal drusenoid deposits and evolution of outer retinal atrophy in age-related macular degeneration. *Ophthalmol Retin*. 2020;4:274–283.
26. Xu L, Blonska AM, Pumariega NM, et al. Reticular macular disease is associated with multilobular geographic atrophy in age-related macular degeneration. *Retina*. 2013;33:1850–1862.
27. Marsiglia M, Boddu S, Bearelly S, et al. Association between geographic atrophy progression and reticular pseudodrusen in eyes with dry age-related macular degeneration. *Invest Opthalmol Vis Sci*. 2013;54:7362.
28. Pumariega NM, Smith RT, Sohrab MA, LeTien V, Souied EH. A prospective study of reticular macular disease. *Ophthalmol*. 2011;118:1619–1625.
29. Spaide RF, Yannuzzi L, Freund KB, Mullins R, Stone E. Eyes with subretinal drusenoid deposits and no drusen: progression of macular findings. *Retina*. 2018;00:1–15.
30. Curcio CA, Messinger JD, Sloan KR, McGwin G, Medeiros NE, Spaide RF. Subretinal drusenoid deposits in non-neovascular age-related macular degeneration: morphology, prevalence, topography, and biogenesis model. *Retina*. 2013;33:265–276.
31. Curcio CA, Sloan KR, Kalina RE, Hendrickson AE. Human photoreceptor topography. *J Comp Neurol*. 1990;292:497–523.
32. Reiter GS, Told R, Baumann L, Sacu S, Schmidt-Erfurth U, Pollreisz A. Investigating a growth prediction model in advanced age-related macular degeneration with solitary geographic atrophy using quantitative autofluorescence. *Retina*. 2019:1.
33. Sayegh RG, Sacu S, Dunavölgyi R, et al. Geographic atrophy and foveal-sparing changes related to visual acuity in patients with dry age-related macular degeneration over time. *Am J Ophthalmol*. 2017;54:739–745.
34. Schmidt-Erfurth U, Klimscha S, Waldstein SM, Bogunović H. A view of the current and future role of optical coherence tomography in the management of age-related macular degeneration. *Eye*. 2017;31:26–44.
35. Schmidt-Erfurth U, Waldstein SM, Klimscha S, et al. Prediction of individual disease conversion in early AMD using artificial intelligence. *Invest Ophthalmol Vis Sci*. 2018;59:3199–3208.
36. Seebock P, Waldstein SM, Klimscha S, et al. Unsupervised identification of disease marker candidates in retinal OCT imaging data. *IEEE Trans Med Imaging*. 2019;38:1037–1047.
37. Shen L, Liu F, Grossetta Nardini H, Del Priore L V. Natural history of geographic atrophy in untreated eyes with nonexudative age-related macular degeneration. *Ophthalmol Retin*. 2018;2:914–921.
38. Shen LL, Sun M, Khetpal S, Grossetta Nardini HK, Del Priore L V. Topographic variation of the growth rate of geographic atrophy in nonexudative age-related macular degeneration: a systematic review and meta-analysis. *Invest Ophthalmol Vis Sci*. 2020;61:2.
39. Monés J, Biarnés M. The rate of progression of geographic atrophy decreases with increasing baseline lesion size even after the square root transformation. *Transl Vis Sci Technol*. 2018;7(6):40.
40. Shen LL, Liu F, Nardini HG, Del Priore L V. Reclassification of fundus autofluorescence patterns surrounding geographic atrophy based on progression rate. *Retina*. 2019;39:1829–1839.

Investigative Ophthalmology & Visual Science

41. van Grinsven MJJP, Buitendijk GHS, Brussee C, et al. Automatic identification of reticular pseudodrusen using multimodal retinal image analysis. *Invest Ophthalmol Vis Sci*. 2015;56:633–639.
42. Lindner M, Böker A, Mauschitz MM, et al. Directional kinetics of geographic atrophy progression in age-related macular degeneration with foveal sparing. *Ophthalmol*. 2015;122:1356–1365.
43. Sohn EH, Flamme-Wiese MJ, Whitmore SS, et al. Choriocapillaris degeneration in geographic atrophy. *Am J Pathol*. 2019;189:1473–1480.

Supplementary Material

Supplementary Video. Process of the 3-point registration technique used to overlap fundus autofluorescence (FAF) to infra-red (IR) images. Junctional zone (*green*) borders were marked on OCT and finally transferred to the registered FAF image.

Investigative Ophthalmology & Visual Science